

## CRACKS AND FATIGUE REMAINING LIFE ASSESSMENT OF ROLLING BEARINGS

M.Sc., João Guilherme Brigoni Massoti, [joao.massoti@skf.com](mailto:joao.massoti@skf.com)

SKF do Brasil, Cajamar/SP – Brazil

Ph.D., Cláudio Ruggieri, [claudio.ruggieri@usp.br](mailto:claudio.ruggieri@usp.br)

University of São Paulo, EPUSP, São Paulo/SP – Brazil

**Abstract.** This work presents the main phenomenon that governs the crack propagation in bearing rings, through the application of Linear Elastic Fracture Mechanics (LEFM) and Fatigue concepts. The complex stress state acting on the bearing ring produces a mixed-mode load over the crack faces. The proposed bearing problem considers a tensile mode and pure shear mode in the plane of the defect, both under a cyclic regime. The stress intensity factor  $K$  and the  $J$ -integral parameters define the fracture conditions and suffice to characterize the severity of cracks developed in bearing rings. The procedure for defect assessment is based on the application of different failure criteria. Using the parameters,  $K$  and  $J$ , coupled to the defect assessment procedures, it is possible to estimate the remaining fatigue life, through models that describe the crack propagation rate. The results indicate that the mixed-mode loading considered in this work is one of the most important parameters in nucleation and propagation of bearing defects and are responsible for a significant reduction in the original estimation of fatigue life.

**Keywords:** Bearings, Stress Intensity Factors, Mixed-Mode, Fatigue

### 1. INTRODUCTION

The current situation in industry is heavily focused on "Reliability", i.e., the definition of how a given asset can operate without failure for a set period of time under certain operating conditions. This indicates that the industry is not only interested in the life of machines and components, but also in the knowledge that they may fail prematurely.

Typically, this approach is practiced by maintenance teams and nowadays the variety of techniques for condition monitoring is quite wide. Among the most common predictive techniques are highlighted vibration analysis, thermography, ultrasound and lubricant analysis. In addition, these techniques allow monitoring the evolution of a particular flaw in the initial stage such as occurs, for example in bearings.

Rarely bearings meet the estimated life cycle, i.e., the incidence of premature failures in this type of component in the industrial segment is quite common as shown in Figure 1. Only 08% of bearings reach the estimated service life, which natural failure mode would be the sub-surface fatigue (SKF Group, 1994). This happens by the action of external factors such as those cited in Figure 1, generating distinct failure modes, or even by an inadequate definition of the design parameters.

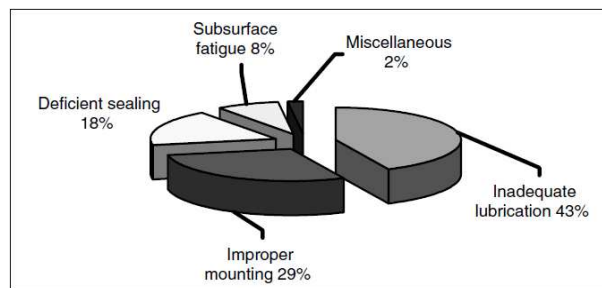


Figure 1. Occurrence of bearing failures, divided by origin (Harris, Kotzalas, 2007a)

The motivation for this study follows exactly the theme above, where from the evaluation of defects that lead to catastrophic failure, it is possible to obtain preliminary data as to its severity, providing support for decision making involving the replacement of components with a more technical background.

As there is a great variety of bearing designs and failure modes as well, this paper will restrict itself to the study of single row cylindrical roller bearings and the surface crack type defect, generated from the inner raceway surface fatigue. This approach is justified by the high demand of this bearing design, and by the high incidence of premature failure due to inadequate lubrication (43%), which predominant mode of failure would be the surface fatigue.

The purpose of this study is, therefore, propose procedures and analysis tools for bearings defects, based on Fracture Mechanics and Fatigue concepts, encompassing basically the crack severity assessment and later, if possible,

the estimation of the bearing fatigue remaining life. In addition, it is intended also to quantify the forces that are significant for crack propagation, thus providing tools for bearing development.

## 2. METHODOLOGY

### 2.1. Problem Statement

Several factors affect the surface crack growth in problems involving rolling contact forces. This includes the shape and slope of the defect, the hoop stress field originated from the rotation and bearing adjustment, the Hertzian contact force, the lubricant pressure acting on the crack walls, the shear stresses arising from sliding contact, and friction between the walls of the crack (Ballarini, Hsu, 1990). These conditions induce a complex stress state in the bearing ring, which culminates in a mixed mode loading problem (Mendelson, Ghosn, 1986).

Several studies have been conducted, aiming a better understanding of each of these factors. Despite being three-dimensional problem, much of the analysis available in the literature is two-dimensional. In the development of fatigue cracking, few information on this phenomenon in mixed mode loading are available in the literature.

In this study, we propose an analytical model for obtaining the stress intensity factors and this in a first moment, neglects some of the factors set forth above, during the determination of the stress field. For example, the friction between the walls of the crack, which would culminate in a slowing growth, the effect of lubricant pressure, considering that the compressibility, inertia and oil viscosity act minimizing the pressure over the defect, and contact sliding, by assuming a pure rolling interaction between rollers and raceway (Ballarini, Hsu, 1990). The latter can be partially checked if the applied load meets the requirements of "minimum load" defined by the bearing manufacturer (SKF Group, 2005).

The centrifugal force that arises from the rolling elements is also neglected. This is because the rotation is relatively low and therefore not provides a force of significant magnitude (Harris, Kotzalas, 2007a). In addition, thermal and dynamic effects are not considered and the influence of oil film on the Hertzian pressure distribution as well.

Table 1 sets out the bearing specification to which the model will be applied - NU 322. This type of component is widely used in medium size electric motors, responsible to drive centrifugal pumps, vacuum pumps, fans, etc. The specified bearing, when introduced into the model, will be subjected to typical operating conditions of electric motors, 1200 rpm of the inner ring and a radial force in the most loaded rolling element of 10 kN, 15 kN and 20 kN. According to SKF Group (2005), these values are considered moderate when applied to the reference bearing. In addition, the component will also be subjected to a more severe condition, with a load of 40 kN and a less severe, with 5 kN. The relationship between the total radial load ( $F_r$ ) applied to the bearing, and their resultant force on the most loaded rolling element ( $F_r$ ) is given by eq. (1) (Harris, Kotzalas, 2007b). Equation (1) is only valid for normal internal radial clearance, which  $Z$  is the number of rolling elements and  $\zeta$  the contact angle between roller and raceway.

$$F_r = \frac{F_t \cdot Z \cdot \cos \zeta}{5} \quad (1)$$

The defect type planar crack will be induced on the surface of the inner ring, it is figured by the ratio of crack length and width of the specimen  $a/W=0,1$ , and the direction perpendicular to the rolling surface. This configuration is common in crack problems involving bearings, based on the work of Mendelson and Ghosn (1986), and Ballarini and Hsu (1990).

As mentioned, the analysis of defects in bearings is a mixed mode loading problem. This condition is imposed mainly by the multiaxial stress field, derived from the Hertzian contact forces and hoop stress, originated from the bearing adjustment and rotation speed. These are the most important loads to consider in the analysis. Following, we present an analytical model to determinate the multiaxial field, which then supports the stress intensity factors calculation.

Table 1. Cylindrical roller bearing NU 322 (SKF Group, 2005)

Description	Data
Number of rolling elements	$Z = 14$
Rolling elements diameter	$D_{we} = 34,000$ mm
Rolling elements length	$L_{we} = 34,000$ mm
Shaft inner radius	$a_s = 0,000$ mm
Shaft outer radius	$b_s = 55,024$ mm
Inner ring bore radius	$a_i = 54,995$ mm
Inner ring raceway radius	$b_i = 71,500$ mm
Outer ring raceway radius	$a_o = 105,500$ mm
Outer ring outside radius	$b_o = 120,000$ mm

## 2.2. Multiaxial loading

Regarding the hoop stress, Saada (1983) defines it as a rotation and interference fit dependent. The eq. (2) shows this dependence for application via the imperial system of units.  $\sigma_{\theta\theta}$  is the hoop stress,  $\rho_m$  the bearing steel density,  $\nu$  the Poisson's ratio,  $\omega$  the angular velocity and  $P$  the mounting pressure between inner ring and shaft, which also comes from Saada (1983).  $r_i$  is a random radius in the inner ring.

$$\sigma_{\theta\theta} = \frac{3+\nu}{8} \cdot \rho_m \cdot \omega^2 \cdot \left[ b_i^2 + a_i^2 + \frac{a_i^2 \cdot b_i^2}{r_i^2} - \frac{1+3\nu}{3+\nu} \cdot r_i^2 \right] + P \cdot \frac{(b_i/r_i)^2 + 1}{(b_i/a_i)^2 - 1} \quad (2)$$

From eq. (2), it appears that the  $\sigma_{\theta\theta}$  values vary along the radius of the inner ring between 65.8 and 88.5 MPa. This  $\sigma_{\theta\theta}$  value is smaller as  $r_i$  decreases, due to the press fit reduction and a smaller centrifugal effect.

The next step is to find the stresses arising from contact between rolling element and the raceway. This will apply the theory developed by Heinrich Rudolph Hertz in 1882, which is based on the condition that the dimensions of the contact area are smallest compared with the size of solids in contact and the curvature radius, the forces applied are perpendicular to the surface and deformations occur in the elastic field (Harris, Kotzalas, 2007b).

In this context, it appears that the Hertz theory covers reasonably well the problem postulate, considering only radial forces, which results in a stress field that belongs within to the elastic field. There are other theories more precise and complex that can be used to find the pressure for different contact patterns, for example, applications with misalignment forces. One of the most used today is called *Slicing Technique* (Harris, 1969), however, is not discussed in this work.

The proposed model neglects the curvature radius of the raceway, bringing it to a uniform flat plate. This is because the relationship between the thickness of the ring and the inner radius of the raceway is small. Moreover, in view of the transverse uniformity of stress distribution in Figure 2-b, the model will be restricted to two dimensions.

According to Smith and Liu (1953), the stress components are defined as  $\sigma_x$ ,  $\sigma_y$ ,  $\sigma_z$  and  $\tau_{xz}$ . For the proposed problem, the equation for components in plane strain state is given by eqs. (3) and (4).

$$\sigma_x = -\frac{P_0}{\pi} \cdot \left\{ \left( b_h^2 + 2 \cdot x^2 + 2 \cdot z^2 \right) \cdot \frac{z}{b_h} \cdot \Psi - 2 \cdot \pi \cdot \frac{z}{b_h} - 3 \cdot x \cdot z \cdot \psi + \mu_f \cdot \left[ \left( 2 \cdot x^2 - 2 \cdot b_h^2 - 3 \cdot z^2 \right) \psi + 2 \cdot \pi \cdot \frac{x}{b_h} + 2 \cdot \left( b_h^2 - x^2 - z^2 \right) \cdot \frac{x}{b_h} \cdot \Psi \right] \right\} \quad (3)$$

$$\tau_{xz} = -\frac{P_0}{\pi} \cdot \left\{ z^2 \cdot \psi + \mu_f \cdot \left[ \left( b_h^2 + 2 \cdot x^2 + 2 \cdot z^2 \right) \cdot \frac{z}{b_h} \cdot \Psi - 2 \cdot \pi \cdot \frac{z}{b_h} - 3 \cdot x \cdot z \cdot \psi \right] \right\} \quad (4)$$

where  $P_0$  is the maximum pressure of the elliptical pressure field,  $\mu_f$  the coefficient of friction and  $b_h$  the minor semi-axis of the ellipse.  $\Psi$  e  $\psi$  are functions of  $x$  and  $z$  coordinates, and of  $b_h$  (Smith, Liu, 1969).

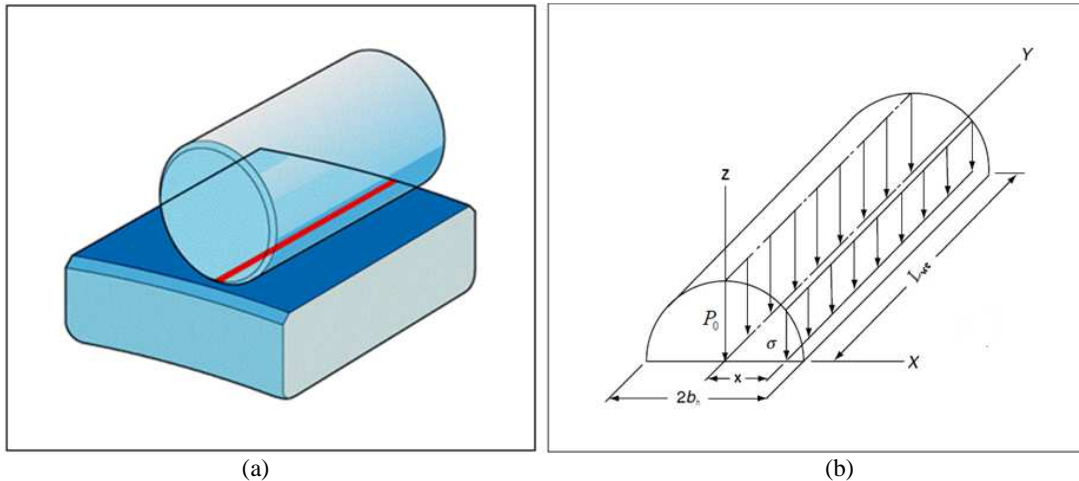


Figure 2. a) Schematic drawing illustrating the contact between rolling element and raceway b) Pressure distribution on the contact area for purely radial loading of pure rolling motion (Harris, Kotzalas, 2007b)

Subsequently, the solution is presented for calculating the maximum pressure  $P_0$  and the radius of the semi-axis of the ellipse  $b_h$ .  $P_x$  is the distribution of contact pressure (Hertz, 1882). This equation is valid only when the length of the contact surfaces is equal. Typically, the application of bearings considers that the Poisson ratio and elasticity modulus of rings and rolling elements are equal.

$$P_x = P_0 \cdot \sqrt{1 - \frac{x^2}{b_h^2}} \quad (5)$$

$$P_0 = \frac{2 \cdot F_t}{\pi \cdot b_h \cdot L_{we}} \quad (6)$$

$$b_h = 2 \cdot \sqrt{\frac{F_t \cdot \left[ \frac{(1 - \nu_1^2)}{E_1} + \frac{(1 - \nu_2^2)}{E_2} \right]}{\pi \cdot L_{we} \cdot \left( \frac{1}{b_i} + \frac{2}{D_{we}} \right)}} \quad (7)$$

It will be considered that during the movement of the rolling element over the defect, the changing in the Hertzian forces pattern is minimal (Ballarini, Hsu, 1990). Figure 3 represents the stress distribution of eqs. (3) and (4). Note that the data shown are normalized, i.e., are valid for any loading on the rolling elements ( $F_t$ ) and therefore any contact area ( $b_h$ ).

Distributions shows the stress values for a given fixed point (zero position on the abscissa axis), depending on the position of the rolling element. Under normal stress  $\sigma_x$ , the highest values are observed with the rolling element on the reference point, and decrease when the roller moves away. In the case of shear stress  $\tau_{xz}$ , there is a rise in values, when the rolling element approaches the point of reference, however, they suffer a reversal sign when the roller crosses from one side to another, reaching zero value exactly on the reference.

The normal stresses are maximum on the surface,  $z=0$ , but the shear stress is null. Its magnitude is maximum on  $z=b_h/2$ , however, as the dimension of depth increases, this value is reduced.

In bearing problems, normally, the tangential forces applied come from normal forces ( $F_t$ ), induced on the raceway by the coefficient of friction  $\mu_f$ . The friction coefficient varies with the lubrication condition, that is, the ability of the lubricant film to separate the surfaces in contact. In applications with partial separation, i.e., where some rough edges still in touch,  $\mu_f \approx 0.1$  (Harris, Kotzalas, 2007a).

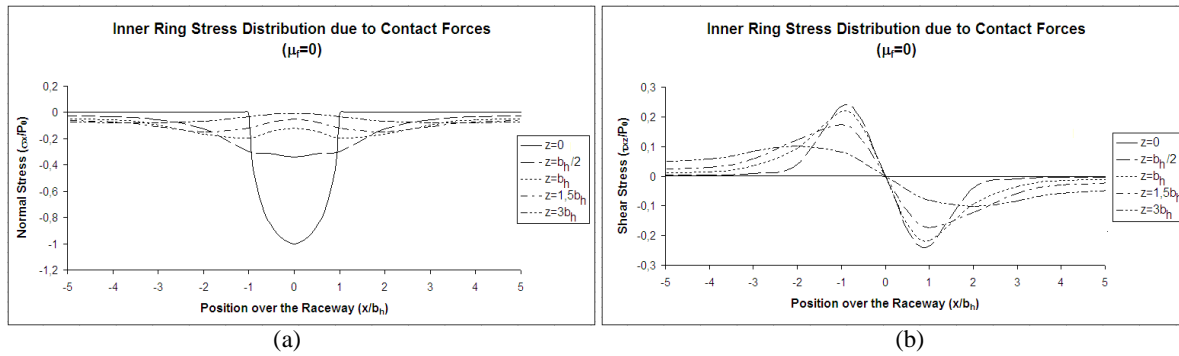


Figure 3. a) Stress distribution  $\sigma_x$  b) Stress distribution  $\tau_{xz}$  in the inner ring to various depths, as a result of contact and movement of the rolling element

### 2.3. Stress Intensity Factors

As mentioned on Section 2.1 and exposed on 2.2, the bearing ring is subjected to multiaxial loading, when in operation. An aggravating of this condition is the fact that loading vary cyclically with each pass of the rolling elements. characterized in a way, the failure mode that we intend to study in this article, the surface fatigue. From the nucleation of a defect in the inner ring raceway, it is possible to estimate the remaining fatigue life of this component, until the defect reaches a critical size, which will result in unstable crack propagation and subsequent rupture. To this end, it is necessary to develop a method for calculating stress intensity factors, which serve as criteria to evaluate the severity of the defect and calculation of remaining life.

The method of stress intensity factors calculation is valid for surface defects nucleated at the center of the inner ring raceway, assuming the existence of plane strain state, as illustrated in Figure 4. The calculation parameters are the same as set out in sections 2.1 and 2.2, i.e., Hertzian contact forces and hoop stress, originated from bearing adjustment and rotation. By neglecting the curvature radius, the two-dimensional model applied is approximated to a flat plate, uniform, over which moves a cylinder, simulating the roll of the rolling element along the inner ring - Figure 4 (Mendelson, Ghosn, 1986).

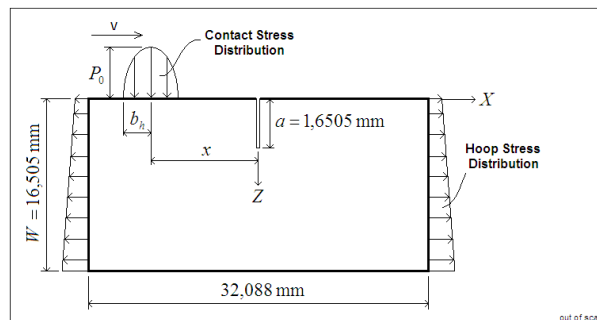


Figure 4. Illustrative model of the bearing inner ring, exposing the component settings and loading profile

Looking at the layout of the defect and the associated stress, it is concluded that the open mode is associated with the normal stresses in the X direction and the pure shear mode with the shear stresses on the XZ plane. For the problem of Figure 4 there is no incidence of the shear mode in longitudinal directions (Massoti, 2011). In this context, the determination of stress intensity factor for mode I is influenced by the Hertzian contact forces, as by hoop stresses. The stress intensity factors are additive, so  $K_I$  can be calculated separately for each type of loading and then added to. The portions  $K_{I1}$  and  $K_{I2}$  of which come from the Hertzian contact forces are defined by eq. (8) (Tada et al., 1985) and the portion of  $K_I$  arising from hoop stresses, by eq. (9) (Anderson, 1995). Previously, the concepts of Linear Elastic Fracture Mechanics has been validated with the data of the proposed problem (Massoti, 2011).

$$\begin{Bmatrix} K_{I1} \\ K_{I2} \end{Bmatrix} = \frac{2}{\sqrt{\pi \cdot a}} \cdot \int_0^a \begin{Bmatrix} \sigma_x \\ \tau_{xz} \end{Bmatrix} \cdot \frac{1}{\sqrt{1-(z/a)^2}} \cdot \begin{Bmatrix} f(z/a) \\ f(z/a) \end{Bmatrix} \cdot dz \quad (8)$$

$$K_I = \frac{F_\theta \cdot f(a/W)}{B \cdot \sqrt{W}} \quad (9)$$

where  $f(z/a)$  and  $f(a/W)$  are functions depending on the loading mode and specimen geometry. In particular,  $f(a/W)$  is only valid to SENT specimen (Anderson, 1995).  $F_\theta$  is the load resulting from  $\sigma_{\theta\theta}$ .

Earlier, the analytical model was validated on the work of Mendelson and Ghosn (1986). The authors applied the Boundary Integral Equation Method to calculate the stress intensity factors of a flat surface crack, placed on the inner race of a high speed radial bearing. Figure 5 presents the stress intensity factors for various loads and conditions proposed, and relationship  $a/W=0,1$ .

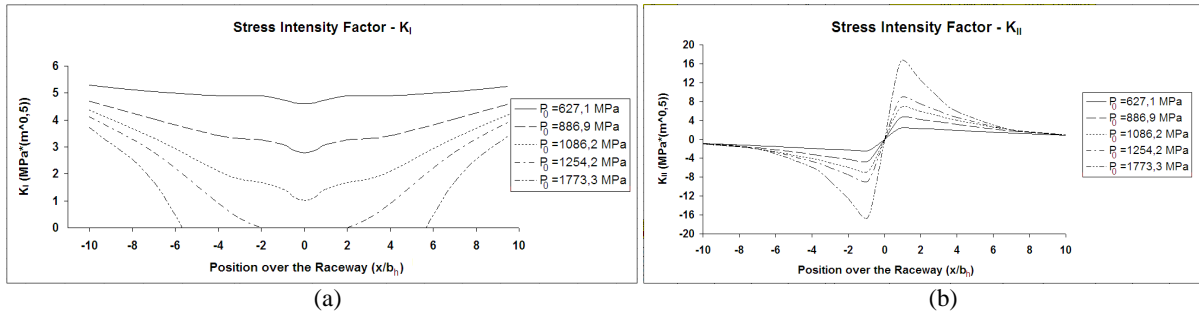


Figure 5. a) Stress intensity factor range  $K_I$  b) Stress intensity factor range  $K_{II}$  on the crack tip, according to the rolling element positions for different loads

Within  $K_I$ , it is noted that the combination of loads, Hertzian contact pressure and hoop stress, generates an interesting effect on the variation of magnitude versus the position of the rolling element. Initially, to positions relatively far from the crack area ( $x/b_h=0$ ),  $K_I$  tends to be equal to the value from the hoop stresses,  $K_I = 6,52 MPa.(m)^{0,5}$ , which is constant and valid for any  $P_0$ . As the rolling element moves in the vicinity of the crack, the  $\sigma_x$  stresses arises from the Hertzian forces, generate a compressive effect on the defect. Thus, there is a decrease in overall value  $K_I$ , so that for values  $P_0 > 1200 MPa$ , no effect of crack opening, when the rolling element lying in the vicinity of the defect, in view of null global values of  $K_I$ .

Another interesting aspect comes from the curve  $P_0=627,1 MPa$ , which  $K_I$  presents a stable behavior along the route considered. Because it is low magnitude loading, the compressive stresses  $\sigma_x$  show little influence on the overall value  $K_I$  of which is basically constituted by the portion of the original hoop stresses. In this case, although the contact pressure is low, it is the case that the crack is subjected to the most significant effect of openness, i.e.,  $K_I$  varying between  $P_0=4,59-6,52 MPa.(m)^{0,5}$ .

In case of  $K_{II}$  the variation of magnitude much resembles the behavior of  $\tau_{xz}$  (Figure 3b), i.e.,  $K_{II}$  decreases dramatically when the rolling element moves away from the crack, but quickly gains magnitude, as it approaches and reaches its maximum value in the region  $x/b_h=\pm 1,0$ . Notice the reversal in the direction of shear stress and consequently the signal  $K_{II}$  when the roller moves into the vicinity of the crack, passing from one side to another of the defect. The change in signal indicates only that the sense of shear was changed, the effect is maintained over the defect.

$K_{II}$  has zero value when the roller is positioned exactly on the crack, indicating no shear, as the Hertzian contact forces are distributed equally on both sides. Opposite to that observed to  $K_I$ ,  $K_{II}$  presents greater magnitudes as greater the  $P_0$  value. In this case, the maximum is for  $P_0=1773,3 MPa$ ,  $x/b_h=\pm 1,0$  and  $K_{II}=\pm 16,82 MPa.(m)^{0,5}$ .

$K_I$  and  $K_{II}$  variations illustrate again the existence of cyclic loading on the bearing. This reinforces the prevalence of fatigue on the bearing service life. According to Hertzberg (1996),  $K_{IC}$  value for the bearing steel AISI 52100 is about  $14,3 MPa.(m)^{0,5}$ .

#### 2.4. Defects Assessment and Failure Criteria

A component fails locally for a given condition of stress and strain, also defined by a critical stress intensity factor  $K_C$  (Anderson, 1995). In the case of bearing steel AISI 52100,  $K_C$  is fairly available for the three modes of crack loading. Normally only  $K_{IC}$  is available in the literature.

In previous sections, the crack is considered subject to mixed mode loading, i.e., mode I and II. In this case, it is necessary to apply models to assess the severity of defects in mixed mode, just considering  $K_{IC}$  as parameter. According to Pook (2010), these models express the mixed mode loading in the form of equivalent mode I, i.e., an equivalent driving force  $J_{eq}$  originated from  $J(K_I, K_{II}, K_{III})$  to compare with the fracture toughness in mode I.

Several models are available under the name “Failure Criteria”, with no great similarity between them. In fact, as the name implies, these criteria are adopted differently in each model. For the current case, three models will be applied to the analysis of defect severity, Coplanar Propagation Criteria (Thiemeier et al., 1991), Maximum Hoop Stress Criteria (Thiemeier et al., 1991) and finally, the criteria adopted by the European Fitness-for-Service Network (FITNET, 2006).

Based on the data of Figure 5, the three methods are applied separately and the results are shown in Figure 6. By analyzing the curves, it appears that only for  $P_0=1773,3 \text{ MPa}$  in all criteria, the stress field generated involves developing of a driving force greater than the fracture toughness of the material. Thus, the risk of fracture becomes imminent at the given moment of analysis, and crack is classified as critical. So, for all loads is possible to calculate the remaining fatigue life, except for the critical case where the propagation is unstable and controlled by  $K_{IC}$ , Region III of the curve  $da/dN$  vs.  $\Delta K$  (Dowling, 1999). Further details in the next section.

Previously mentioned, the loading on the crack varies with the position of the rolling element. In this case, it appears that the driving force is maximum at  $x/b_h = \pm 1,0$ , independent of  $P_0$ . A comparative analysis of the curves and the assessment line, allows to notice that the crack severity of the FITNET criteria is superior if compared to the levels stipulated in other criteria, especially between  $x/b_h = \pm 0,5$  and  $\pm 4,0$ . In this context, there are two ways of analysis, i.e., one related to a possible conservatism of FITNET model and another, as resemblance to reality.

From the equivalent parameters of fracture is possible to determinate the critical crack size, according to the three failure criteria. The calculation comes from the application of eq. (9), replacing  $\sigma_{\theta\theta} = \sigma_{\theta\theta(\max)}$ . The presence of  $f(a/W)$  requires that the calculation is interactive, from the variation of crack length  $K_I$  up to  $K_{IC}$ . The following Table 2 lists the  $a_C$  values for the various criteria.

The smallest critical crack lengths comes from FITNET Criteria, which according to the comments above, would be an expected result because it is the criteria which initial severity of the defect, was ranked the highest. The larger critical crack lengths results from the Coplanar Propagation Criteria. For small loads,  $P_0=627,1 \text{ MPa}$  and  $P_0=886,9 \text{ MPa}$  the Maximum Hoop Stress and FITNET Criteria are equivalent, i.e., the critical crack lengths are identical.

These results demonstrate the relevance of the driving force under mode II loading, which is somewhat more emphasized by FITNET through their formulations (FITNET, 2006). This aspect is reinforced by the analysis given in section 2.3, which appears that the  $K_I$  stress intensity factors of smaller magnitude, comes from the contact forces of greatest magnitude, and goes against to what happens under mode II and showed on Figure 6.

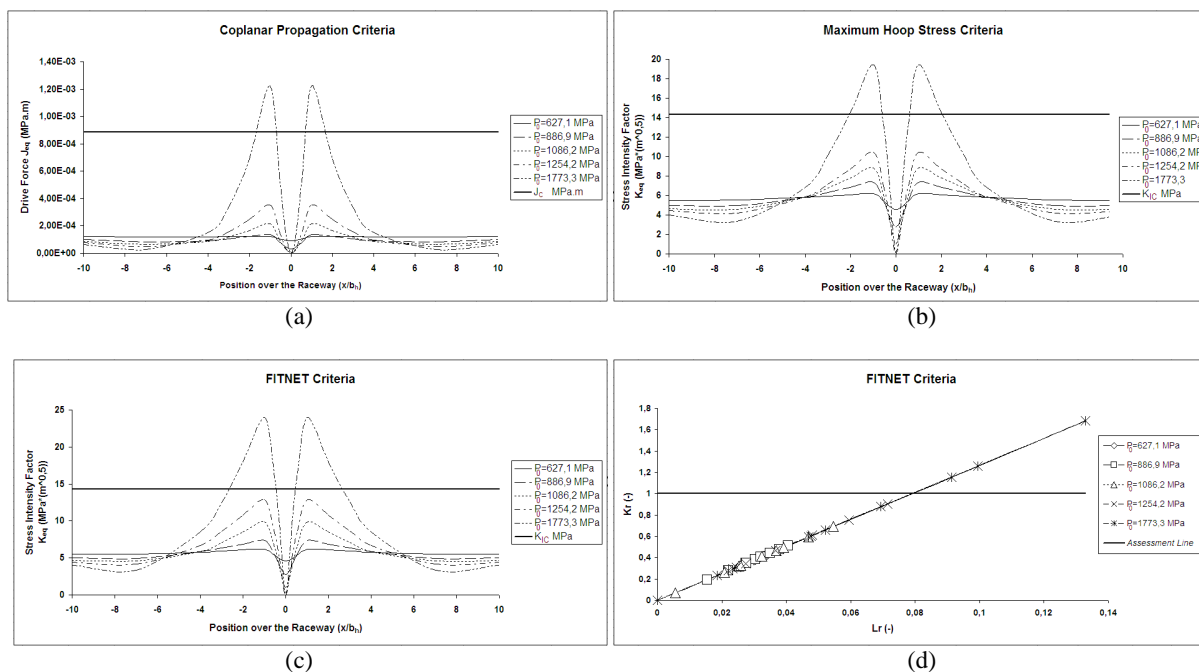


Figure 6. a) Driving force range  $J_{eq}$  b)  $K_{eq}$  range c)  $K_{eq}$  range on the crack tip, according to the rolling element positions, for different loads. Assessment according to  $J_c$  e  $K_{IC}$  d)  $K_r \times L_r$  range for different loads, according to FITNET criteria (FITNET, 2006)

Table 2. Critical crack length according to failure criteria

$P_0$ (MPa)	$a_C$ (mm) - Coplanar Prop.	$a_C$ (mm) - Max. Hoop Stress	$a_C$ (mm) - FITNET
627,1	5,40	4,95	4,95
886,9	5,20	4,45	4,45
1086,2	4,55	3,90	3,63
1254,2	3,90	3,50	2,97
1773,3	2,40	2,15	1,78

## 2.5. Remaining Fatigue Life Calculation

The calculation of the remaining fatigue life is based on the previous incidence of a defect on the inner ring raceway. The remaining life is defined as the time or number of cycles for the initial crack reach the critical size. Initially, to have a considerable remaining life, the driving force acting on the crack, must be less than the fracture toughness of the material. Otherwise, the crack propagation rate is relatively high and unstable, resulting in a negligible number of cycles (Dowling, 1999).

The proposed model is valid for region II of the  $da/dN$  vs.  $\Delta K$  curve (Dowling, 1999), however, it will also be applied to estimate the number of cycles under unstable propagation, according to results of section 2.4. According to Massoti (2001), the crack propagation rate is above the linear region. All calculations developed in this section are based on results from FITNET Criteria.

The calculation of remaining life is based on two different models. The first is based on a numerical integration of the curve  $dN/da$  versus the instantaneous crack length for constant loading cycle. The second refers to a function of variable amplitude loading (Dowling, 1999).

The use of these methods requires, first, knowledge of the critical crack length, which values come from Table 2, column FITNET. Where  $P_0=1773,3$  MPa the calculation indicates a critical crack length bigger than the original, already demonstrated as critical in Section 2.4. This is because depending on the position of the rolling element, the driving force does not exceed the value  $14,3$  MPa.(m)<sup>0,5</sup>. In this case, the estimated remaining fatigue life is based on the value of Table 2.

In general, the first and second models are defined as eqs. (10) and (11), respectively (Dowling, 1999). Such equations were previously formatted to be implemented in the proposed problem.

$$RL = \frac{1}{2} \cdot \int_{a_j}^{a_c} \left( \frac{dN}{da} \right) da \quad (10)$$

$$RL = \frac{1}{3} \cdot \frac{a_c^{(1-m/2)} - a_j^{(1-m/2)}}{C \cdot [f(a/W) \cdot \Delta \sigma_e \cdot \sqrt{\pi}]^m \cdot (1-m/2)} \quad (11)$$

where the following values were considered for the constants  $C$  e  $m$  respectively,  $5,87 \cdot 10^{-13}$  m/ciclo / (MPa. $\sqrt{m}$ )<sup>m</sup> and 4,78, adjusted properly by  $\sigma_{\min} / \sigma_{\max}$  (Tanaka, Akiniwa, 2002).  $\Delta \sigma_e$  is the equivalent stress range.

From the models, follow in Table 3 the remaining fatigue lives for each condition. The results indicate that the magnitude calculated is the same in both methods. For the two lower loads, the variation is small among them, and for larger loads is greater.

The assessment between models allows to indicate some advantages and disadvantages of each. For example, considering the load profile, the second method enables a more detailed reading of the curve than the first, in order to divide the curve of load on different regions. Therefore, the variation of the driving force for the passage of the rolling element is better characterized. On the other hand, the first model allows for the calculation to compute the rate change  $dN/da$  as function of instantaneous crack size. This is possible because of the term  $a_j$ .

Table 3. Remaining fatigue life of NU 322 (roller movement – load cycles)

$P_0$ (MPa)	$RL$ (Numerical Int.)	$RL$ (F.V.A)
627,1	22.817.688	21.516.570
886,9	1.190.854	1.405.796
1086,2	117.480	193.893
1254,2	24.522	39.073
1773,3	375	573

The results above were compared to similar simulations ( $P_0=886,9$  MPa) made by Mendelson and Ghosn (1986). The results demonstrate equivalence in magnitude between the values of the two studies and therefore are of great value to the goals.

### 3. CONCLUSION

At the end of the study, it's possible to enumerate the following conclusions, according to the order of the topics covered:

- The complex stress state induced in the bearing ring culminates in mixed mode loading on the crack walls;
- $\sigma_x$  and  $\tau_{xz}$  are one of the most important parameters to consider in the nucleation and propagation of cracks in bearing rings. In general, these components originate from the rotation and bearing adjustment, and the Hertzian contact forces between rollers and raceways;
- In the proposed problem, the mixed mode loading is defined by the presence of the open mode and pure shear in the plane of the defect;
- The cyclical behavior of  $K_I$  and  $K_{II}$  (Figure 5) reinforces the prevalence of fatigue on the bearing life;
- The stress intensity factor  $K$  and the  $J$ -integral parameters define the fracture conditions and suffice to characterize the severity of cracks developed in bearing rings;
- For low magnitude loads ( $P_0=627,1$  MPa) the open mode contributes more effectively to the crack propagation than the shear mode. As for loads of medium and large magnitudes, this condition changes and mode II becomes progressively more relevant. This can be evidenced by the results presented in section 2.4, where it appears that the regions of higher  $K_{eq}$  coincide with the higher  $K_{II}$ ;
- The three failure criteria presented converge to the same result of defect severity. By the analysis performed, it is noted that the FITNET Criteria indicated greater severity of the crack than the other, and this aspect seems to be more real;
- The remaining fatigue life calculation showed that both models used, converge on the same scale of values;
- The short periods of remaining life  $RL$  indicates that to achieve values of greater magnitude, the bearing must be subjected to smaller loads ( $F_r$ ) and reduced number of cycles ( $n$ );
- The  $RL$  values are not absolute, because it comes from several simplifying assumptions, and should only be used as references in order of magnitude;
- The analysis carried out are of great value to the development of new materials and bearing designs, as well as contribution to the reliability analysis related to bearings;
- As next step for this study, the present methodology shall be validated experimentally.

#### 4. REFERENCES

- Anderson, T.L., 1995. "Fracture Mechanics – Fundamentals and Applications", 2nd Edition, CRC Press, Boca Raton.
- Ballarini, R., Hsu, Y., 1990. "Three-Dimensional Stress Intensity Factor Analysis of a Surface Crack in a High-Speed Bearing", *International Journal of Fracture*, Vol. 46, pg. 141-158.
- Dowling, N.E., 1999. "Mechanical Behavior of Materials", 2nd Edition, Prentice Hall, USA.
- European Fitness-for-Service Network, FITNET, 2006. "Fitness-for-Service Procedure", MK7.
- Harris, T.A., 1969. "The Effect of Misalignment on the Fatigue Life of Cylindrical Roller Bearings Having Crowned Rolling Members", *ASME Journal of Lubrication Technology*, No. 2, pg. 294-300.
- Harris, T.A. and Kotzalas, M.N., 2007. "Advanced Concepts of Bearing Technology", 5<sup>th</sup> Edition, CRC Press, Taylor & Francis Group.
- Harris, T.A. and Kotzalas, M.N., 2007. "Essencial Concepts of Bearing Technology", 5<sup>th</sup> Edition, CRC Press, Taylor & Francis Group.
- Hertz, H., 1882. "Über Die Berührung Fester Elastischer Körper, *J. Reine Und Angewandte Mathematik*", Vol. 92, pg. 156-171.
- Hertzberg, R., 1996. "Deformation and Fracture Mechanics of Engineering Materials", 4<sup>th</sup> Edition, Wiley, New York.
- Massoti, J.G.B., 2011. "Metodologia para Análise de Defeitos em Rolamentos e Cálculo da Vida Remanescente à Fadiga", *Dissertação de Mestrado, Universidade de São Paulo*.
- Mendelson, A., Ghosn, L.J., 1986. "Analysis of Mixed-Mode Crack Propagation Using the Boundary Integral Method", *NASA Contractor Report 179518, Lewis Research Center*.
- Pook, L.P., 2010. "Five Decades of Crack Path Research, *Engineering Fracture Mechanics*", Vol. 77, pg. 1619-1630.
- Saada, A.S., 1983. "Elasticity, Theory and Applications", Robert E. Krieger Publishing Company Inc.
- SKF Group, 1994. "Bearing Failures and Their Causes", *Product Information PI 401 E, Gothenburg*.
- SKF Group, 2005. "General Catalogue", 6000 EN, Gothenburg.
- Smith, J.O., Liu, C.K., 1953. "Stress Due to Tangential and Normal Loads on an Elastic Solid With Application to Some Contact Stress Problems", *Journal of Applied Mechanics*, Vol. 20, No. 2, pg. 157-166.
- Tada, H., Paris, P.C., Irwin, G.R., 1985. "The Stress Analysis of Cracks Handbook", 2nd Edition, Paris Productions, St. Louis.
- Tanaka, K., Akiniwa, Y., 2002. "Fatigue Crack Propagation Behaviour Derived from S-N Data in Very High Cycle Regime", *Fatigue and Fracture of Engineering Materials and Structures*, Vol. 25, pg. 775-784.
- Thiemeier, T., Brückner-Foit, A., Kölker, H., 1991. "Influence of the Fracture Criterion on the Failure Prediction of Ceramics Loaded in Biaxial Flexure", *Journal of American Ceramic Society*, Vol. 74, pg. 48-52.

#### 5. RESPONSIBILITY NOTICE

The authors are the only responsible for the printed material included in this paper.